Original Article

Lipidome of narrow-band ultraviolet B irradiated keratinocytes shows apoptotic hallmarks

Adam Reich[1]*, Dominik Schwudke[2,4]*, Michael Meurer[3], Bodo Lehmann[3] and Andrej Shevchenko[2]

[1]Department of Dermatology, Venereology and Allergology, Wroclaw Medical University, Wroclaw, Poland;

[2]MPI of Molecular Cell Biology and Genetics, Dresden, Germany;

[3]Department of Dermatology, Carl Gustav Carus Medical Faculty, University of Technology, Dresden, Germany;

[4]National Centre for Biological Sciences, Tata Institute of Fundamental Research GKVK, Bellary Road, Bangalore, India

Correspondence: Adam Reich, MD, PhD, Department of Dermatology, Venereology and Allergology, Wroclaw Medical University, Ul. Chalubinskiego 1, 50-368 Wroclaw, Poland, Tel.: 48 71 7842288, Fax: 48 71 3270942, e-mail: adi_medicalis@go2.pl

These two authors contributed equally to this study.

Abstract

Background: UV light triggers a variety of biological responses in irradiated keratinocytes that might be associated with global perturbation of their lipidome. However, lipids that are specifically affected and the exact molecular mechanisms involved remain poorly understood.

Objectives: To characterize time-dependent changes of the lipidome of cultured keratinocytes induced by narrow-band ultraviolet B (NB-UVB) irradiation.

Methods: Immortalized human keratinocytes (HaCaT) were cultured under standard conditions, irradiated with NB-UVB light (311 nm) at 400 and 800 mJ/cm^2 and collected 1, 2, 3, 6, 12 and 24 h later for lipid extraction. Lipid extracts were separated on silica plates in chloroform/ethanol/water/triethylamine (35:40:9:35) and in n-hexane/ethylacetate (5:1) followed by quantitative shotgun lipidomics analysis.

Results: Irradiation with 800 mJ/cm^2 of NB-UVB altered morphology and lipidome composition of HaCaT cells. Ceramide content increased two-fold 6- and 12-h postirradiation with 800 mJ/cm^2, followed by threefold increase in triacylglycerols (TAGs) that peaked at 24 h. In addition, we observed marked increase of various phosphatidylcholine and phosphatidylethanolamine ethers, whereas phosphatidylcholine-species with short-chain fatty acid moieties decreased. The abundance of other lipid species was altered to lesser extent or remained unchanged.

Conclusions: NB-UVB affected the cellular lipidome of keratinocytes in strictly apoptosis-specific manner.

Key words: apoptosis – keratinocytes – mass spectrometry – shotgun lipidomics – UV light

Introduction

Ultraviolet radiation of the sunlight induces numerous structural and biochemical alterations in the skin in a wavelength-dependent manner (1). For instance, in mice irradiation with UV light with the wavelengths below 310 nm caused epidermal thickening, collagen damage, skin wrinkling as well as skin tumors formation, whereas UV light above 320 nm induced skin sagging (1). In the early 1980s it was suggested that wavelengths between 295 and 313 nm are mainly responsible for the therapeutic effect of UVB, and the range between 310 and 313 nm seems to have the best safety profile (2,3). Therefore, a lamp emitting UVB light at 311–312 nm (known as narrow-band ultraviolet B, NB-UVB) and excluding shorter,

photobiologically more active wavelength range was introduced. NB-UVB is effective in the treatment of numerous skin disorders, including plaque psoriasis, cutaneous T cell lymphomas, atopic eczema, seborrheic dermatitis, pityriasis rubra pilaris, lichen planus, prurigo nodularis, uremic pruritus or even vitiligo (4). As its development, use of NB-UVB is prompted by a combination of its therapeutic efficacy and good safety profile regarding acute adverse events. However, concerns with regard to long-lasting effects were expressed (5,6).

The exact mechanism of NB-UVB action is not fully understood, and it is even unclear whether local or systemic effects are more important (7,8). It was suggested that induction of T cell apoptosis could be a major mechanism of NB-UVB activity, at least in resolving psoriatic

plaques (9). The therapeutic efficacy in psoriasis can also be linked to the observation that dermal T-cells surviving NB-UVB therapy demonstrated reduced capacity to express interferon (IFN)-γ an important proinflammatory cytokine (10). In addition, NB-UVB may have systemic immuno-modulatory effect as peripheral blood mononuclear cells from UVB-treated psoriasis patients were shown to secrete greater amounts of the anti-inflammatory cytokine IL-10, but less IL-1β, IL-2, IL-5 and IL-6 compared with the pretreatment values (11).

Although most NB-UVB effects were attributed to its influence on immune cells, it could also affect the keratino-cytes. NB-UVB induced vitamin D_3 production in irradi-ated keratinocytes was lower, compared with irradiation with 297 nm UVB (12). Epidermal vitamin D_3 has, as was demonstrated *in vitro* and *in vivo*, a distinct antiprolifera-tive and pro-differentiating effects on keratinocytes (13). Besides inhibiting keratinocyte proliferation (14), NB-UVB irradiation led to partial disintegration of the cell membrane and induced externalization of selected nuclear antigens onto keratinocyte surfaces, which reacted with antinuclear antibodies (ANA) collected from patients with lupus erythematosus (15). This indicated that NB-UVB might also induce cutaneous reactions of clinical relevance. At the irradiation doses that were similar to minimal erythema-eliciting dose (MED), it induced apoptosis in cultured keratinocytes (14,16,17). Using atomic force microscopy, we demonstrated previously that NB-UVB strongly altered keratinocyte morphology, both at the cell surface as well as intracellulary (14).

UV light affects cellular lipidomes by activating peroxi-dation of membrane lipids, activation of ceramides (Cer) biosynthesis and releasing arachidonic, dihomo-γ-linolenic and eicosapentaenoic fatty acids from phospholipids (18–21). These studies, however, did not cover the entire cellu-lar lipidome and did not monitor the compositional changes at the level of individual molecular species, which has recently become possible using advanced mass spectro-metric technologies. It is unclear if therapeutic NB-UVB irradiation also inflicts similar oxidative damage of mem-brane lipidome, especially considering morphological changes previously observed in keratinocytes. To address these questions, we have combined thin layer chromato-graphy separation of lipids with high resolution mass spectrometry to assess the changes in the molecular composition of major lipid classes in NB-UVB-exposed keratinocytes.

Methods

Cell culture

The HaCaT cell line, spontaneously transformed, immortal-ized human epithelial cells from adult skin that maintain full epidermal differentiation capacity (kindly provided by Prof. N.E. Fusening, Heidelberg, Germany) (22) was seeded at a density of 3×10^5 cells/cm^2 into 35 mm tissue culture dishes (area $\approx$9.6 cm^2) (Nunc GmbH&Co, Langenselbold, Germany). HaCaT cells were grown for 48 h in DMEM (4500 mg/l glucose + GlutaMax™ I + 110 mg/l pyruvate without Phenol red) (Gibco, Eggenstein, Germany) supple-mented with 5% fetal calf serum (Gibco), 100 U/ml peni-cillin (Gibco) and 100 μg/ml streptomycin (Gibco) at 95% relative humidity, 5% CO$_2$, and 37°C.

Irradiation with UV

Prior to UV irradiation, cells were washed twice with PBS (phosphate buffer saline: 145 mM NaCl, 7.5 mM Na$_2$HPO$_4$, 2.8 mM NaH$_2$PO$_4$) supplemented with 1 mM CaCl$_2$ and 1 mM MgCl$_2$ (PBS/Ca/Mg) and then irradiated at room temperature with 400 mJ/cm^2 and 800 mJ/cm^2 of NB-UVB (1 tube Philips 40 W/TL01, Eindhoven, The Nether-lands) or left non-irradiated for control. The TL01 lamp is characterized by a spectral output of 74% in the narrow waveband between 311 and 313 nm. The detailed spectral irradiance of the lamp used in the current study was pub-lished elsewhere (12). The intensity of irradiation was 0.85 ± 0.04 mW/cm^2 (mean $\pm$ SD). The NB-UVB dose was monitored using a calibrated radiometer (Variocontrol V02.01, Waldmann Medizintechnik, Villingen-Schwennin-gen, Germany). During the irradiation, the buffer tempera-ture was maintained within better than 0.1°C range. After irradiation, the cells were supplied with fresh medium.

Lipid extraction

Lipid extraction was performed according to Bligh and Dyer method (23). Cells were harvested 1-, 2-, 3-, 6-, 12-, and 24-h postirradiation, washed twice with 2 ml ice-cold 155 mM ammonium acetate (NH$_4$OAc) buffer and scraped from the dish in 0.5 ml 155 mM NH$_4$OAc. Next, samples were transferred into a glass tube (Corning GmbH, Kaisers-lautern, Germany) and centrifuged (1000 g for 10 min at 4°C). The supernatant was discarded, cells were resus-pended in 1 ml pure water (4°C) and 3.75 ml of chloro-form/methanol mixture (1:2 v/v) was added to the glass tube. The samples were sonicated for 15 min, 1.25 ml chlo-roform was added, followed by 1.25 ml water, vortexed and centrifuged (1000 g for 10 min at 4°C). The lower phase was collected through protein precipitate with a Pas-teur pipette and transferred into another glass tube. Next, 1.88 ml chloroform was added to the non-lipid residue, vortexed and centrifuged (1000 g). The new lower phase was collected and mixed with the first chloroform phase in the second glass tube. After evaporation, the lipid extract was redissolved in a small volume of chloroform/methanol mixture (2:1). The non-lipid residue was stored for protein determination.

Determination of protein content

The non-lipid residue with the protein disk was dried up and redissolved in 1 ml of 20% SDS. The protein content was estimated based on bicinchoninic acid protocol according to manufacturer instruction (BCA™ Protein Assay Kit, Pierce, Rockford, IL, USA). Briefly, 1 ml of working solution (mixture of 50 parts of BCA™ Reagent A (solution of sodium carbonate, sodium bicarbonate, bicinchonic acid and sodium tartrate in 0.1 M sodium hydroxide) and one part of BCA™ Reagent B (4% cupric sulphate) was added into each 50 μl sample, vortexed and incubated for 30 min at 60°C. Next, the absorbance of each sample was measured at the wavelength $\lambda = 562$ nm and protein content was calculated with the reference to standards of bovine serum albumin that were provided in the kit.

Thin layer chromatography (TLC)

Lipid samples were separated on silica plates (Merck, Darmstadt, Germany). The lipid material loading was normalized using the protein content and was equivalent to 50 μg of the total protein, which corresponded to 5 μg according to previously reported estimates (24). After running two-thirds of the separation distance in chloroform/ethanol/water/triethylamine (35:40:9:35), the plates were dried and separation continued in n-hexane/ethylacetate (5:1) for the full plate distance (25,26). Lipids were detected by charring with 20% sulphuric acid. Finally, TLC plates were scanned, images converted to greyscale and analysed by Image J software available format: (http://rsbweb.nih.gov/ij/). Bands were identified using lipid standards. During the analysis of TLC scans, all peak areas were summed up and considered as 100% of lipid content. The relative content of lipid classes was calculated by normalizing the intensities of corresponding bands to the total intensity of all bands detectable at the TLC image.

Mass spectrometry

Lipid extracts for mass spectrometry were same as for TLC. The total lipid amount in each analysed samples was normalized by the total protein content as described above. Samples were diluted 1:25 by CHCl$_3$/MeOH/2-propanol (1:2:4) containing 7.5 mM NH$_4$OAc. Aliquots (50 μl) was loaded into 96-well plates and sealed with aluminium foil.

Automated shotgun experiments were performed on a LTQ Orbitrap (Thermo Fisher Scientific, Bremen, Germany) and on a modified QSTAR Pulsar I Quadrupole time-of-flight mass spectrometers (MDS Analytical Technologies, Concord, Canada), equipped with NanoMate robotic nanoflow ion sources (Advion BioSciences Ltd, Ithaca, NY, USA) as described previously (27). Lipids were identified and quantified according to Schwudke et al. (28) using LipidX software developed in-house. Briefly, all high resolution survey mass spectra were aligned in a flat file

experiment database. Lipid species were identified using their accurately determined masses whereas intensities were reported for the subsequent quantification. Relative abundances of lipid species were determined by dividing each individual lipid with the total intensity of all identified lipid peaks depicted as relative abundance.

Ceramide species were quantified by targeted MS/MS analysis of all plausible precursors using the long chain base fragment with m/z 264.25 as a reporter ion (29). The total abundance of peaks of all ceramide species was normalized to the abundance of the major lipids PC 34:1 and PC 36:2.

Statistical analysis

Statistical analysis was performed using Statistica 6.0® software (Statsoft, Krakow, Poland). Means and standard deviations were calculated. The differences between compared variables were assessed by ANOVA with a *post hoc* analysis using Tukey's honest significance test. The confidence level of the analysis was set at $\alpha = 0.01$, P values <0.01 were considered significant. Data from at least two independent experiments were used for statistical analysis.

Results

Effects of UVB irradiation on keratinocyte morphology

Corroborating our previous observations (14), we found that low-dose irradiation with 400 mJ/cm^2 of NB-UVB did not markedly influence the growth and morphology of HaCaT cells, whereas doses of 800 mJ/cm^2 of NB-UVB provoked extensive cell changes (Fig. 1). Morphology alterations did not become apparent for at least 2 h postirradiation with 800 mJ/cm^2 when some cells started to retract, before cell death occurred in 3- to 6-h postirradiation (Fig. 1). However, a fraction of cells exposed to 800 mJ/cm^2 of NB-UVB survived until 24-h postirradiation and seemingly increased in size (Fig. 1). This is in accordance with our previous finding that irradiated cells surviving 24-h postirradiation, nearly duplicated their lengths compared with non-irradiated ones (for details see Ref. 14).

Analysis of lipids in UVB irradiated keratinocytes by TLC

We further assessed whether morphology changes observed in irradiated cells were associated with specific changes in their lipidomes. Using the method of TLC as described by Dasgupta and Hogan (25), we detected all major lipid classes in extracts from irradiated keratinocytes and untreated control cells. TLC did not reveal marked alterations of the lipid composition after NB-UVB irradiation with 400 mJ/cm^2, compared with controls (Fig. S1 and
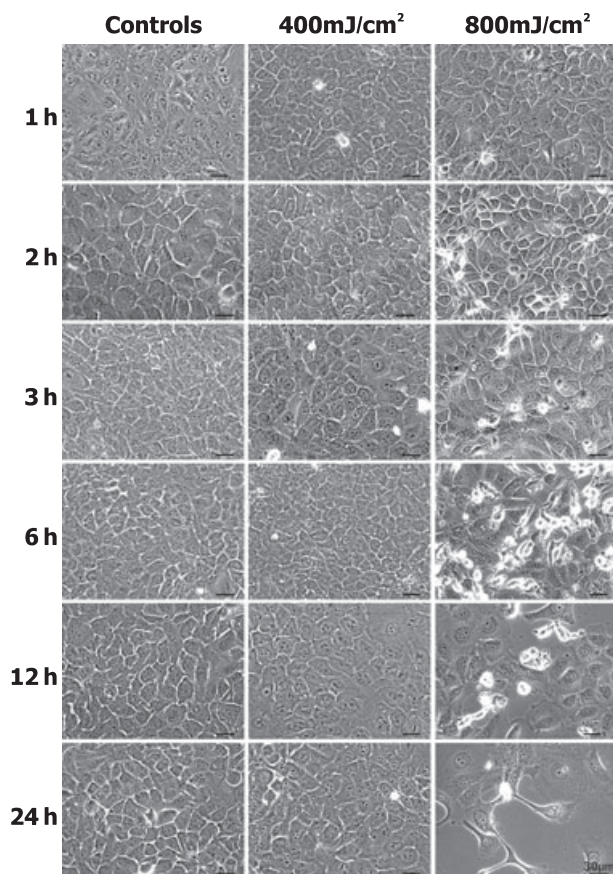
Figure 1. HaCaT cells irradiated with 400 mJ/cm² of narrow-band UVB (second column) did not show marked alterations of culture morphology when compared to control cells (first column). In contrast, irradiation of HaCaT cells with 800 mJ/cm2 of narrow-band UVB (third column) resulted in significant changes in keratinocyte morphology and increased cell death.

Figure 2. (a) Lipid composition of HaCaT cells after irradiation with 800 mJ/cm² of NB-UVB as demonstrated by thin layer chromatography (TLC) Left: original TLC plate scan, right: graphic representations of selected samples as indicated on the right. Upon irradiation, the TAG content increased (double arrowheads). (b–e) Comparison of the abundance of different lipid classes in cells irradiated with 400 mJ/cm² (open bars) and 800 mJ/cm² (black bars) of NB-UVB at different time points after irradiation: TAG (b), Chol (c), PI (d), and SM (e). (b) Significant increase of TAG level in cells irradiated with 800 mJ/cm² 24-h postirradiation compared with all other measurements (*$P < 0.001$). (c) No differences in cholesterol level at different time intervals after irradiation and between various doses of NB-UVB. (d) Significant decrease of PI level in cells irradiated with 800 mJ/cm² 24-h postirradiation compared with cells before irradiation (*$P < 0.01$). (e) Significant decrease of SM level in cells irradiated with 800 mJ/cm² 24-h postirradiation (*$P < 0.01$). Card, cardiolipin; Cer, ceramide; ChE, cholesterol ester; Chol, cholesterol; DAG, diacylglycerol; FFA, free fatty acids; Glc-Cer, glucosyl ceramide; NB-UVB, narrow-band ultraviolet B; PA, phosphatic acid; PC, phosphatidylcholine; PE, phosphatidylethanolamine; PI, phosphatidylinositol; PS, phosphatidylserine; SM, sphingomyelin; TAG, triacylglycerol.

Table S1a). On the contrary, significant changes were observed in cells irradiated with 800 mJ/cm² (Fig. 2a). The most prominent finding was ca. threefold increase of TAG content in 24-h postirradiation (Fig. 2b and Table S1b), which was accompanied by moderate decrease of phosphatidylinositols (PI) and sphingomyelins (SM) (Fig. 2d,e and Table S1). Other lipid classes remained unaffected (Fig. 2c).

Shotgun lipidomics of irradiated keratinocytes

Next we asked, if NB-UVB irradiation altered the molecular composition of the keratinocyte lipidome. To this end, total lipid extracts of irradiated and control cells were subjected to shotgun lipidomics profiling (28). In high resolution mass spectra of total extracts from HaCaT cells (representative examples are shown in Fig. 3) 164 species from 12 lipid classes were identified (Table S2).

Shotgun analysis confirmed that in HaCaT cells TAG were accumulated within 24-h postirradiation with 800 mJ/cm² of NB-UVB (Figs 3 and 4f,g; Table S2),

although their content started to increase already 6-h post-exposure (Fig. 4f,g and Table S2). In addition, we observed marked increase of various PC- and PE-ethers (Fig. 4a,b and Table S2), whereas PC-species with short-chain fatty acid moieties, like PC 30:1, decreased (Fig. 4c–e). Furthermore, Cer 42:1 and Cer 42:2 lipid species increased in abundance (Fig. 4h,i) before the accumulation of TAGs. Further targeted MS/MS analysis revealed that total ceramide levels peaked at 12-h postexposure, while later their content dropped to control levels (Figs. 4h,i and 5; Table S2).
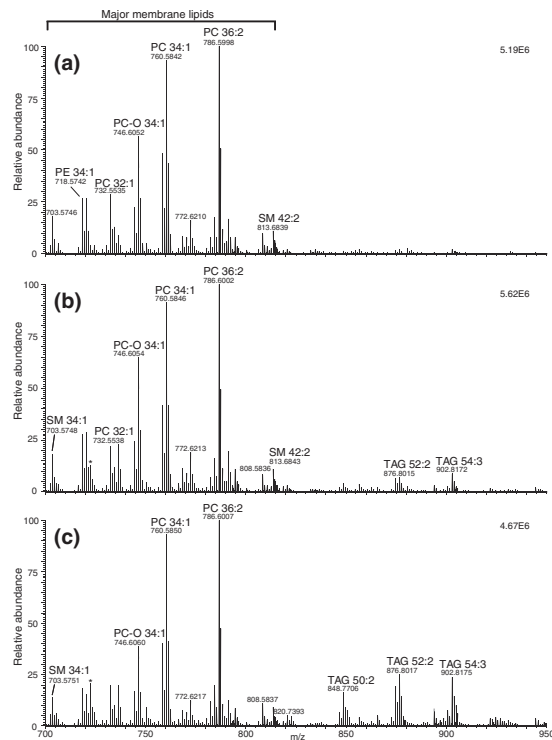
Figure 3. High resolution mass spectra of the total lipid extract from HaCaT cells irradiated with 800 mJ/cm^2 of NB-UVB: PC, phosphatidylcholine; PC-O, 1-alkyl,2-acylglycerophosphocholine; PE, phosphatidylethanolamine; SM, sphingomyelin; TAG, triacylglycerol.

Discussion

Although HaCaT cells are not native keratinocytes, they are a well-established model to study their lipid biology as they have the same total lipid content and distribution of major lipid classes (24). It was also shown that similar doses of NB-UVB were required to induce apoptosis in HaCaT cells compared with NHAK *in vitro* (17).

We demonstrated that NB-UVB altered the lipidome of HaCaT cells and the observed pattern of changes is consistent with unfolding apoptosis. Consistently, Cer levels peaked shortly after the onset of apoptosis, whereas TAGs accumulated at its later stage. Several previous studies also reported accumulation of TAG in various cell types upon different apoptotic stimuli (30–35). This was observed in cells stimulated by free fatty acids and Fas pathway activation. Increased TAGs content is a generally recognized apoptosis marker, which is unrelated to the factors inducing this process. Upon Fas pathway activation, TAG started increasing as early as 1 h after the stimulation together with the loss of mitochondrial transmembrane potential (31,33). Al-Saffar et al. (31) suggested that in Jurkat T cells altered PC metabolism resulted in TAG accumulation. It was found that PC biosynthesis was inhibited during apoptosis at the level of cytidine diphosphate-choline:1,2-DAG choline phosphotransferase and that the accumulation of PC substrates that might activate TAG production (31,36,37). Our data support this notion as the relative abundance of some PC species decreased post-NB-UVB exposure (Fig. 4). It was speculated that TAG accumulation in non-adipose cells might constitute a protective mechanism against apoptosis, as the increased ability to incorporate free fatty acids into TAG decreased the apoptosis ratio and the magnitude of TAG accumulation correlates with cell survival upon exposure to palmitate (32,34). However, the exact mechanism remains controversial as other authors suggested that TAG accumulation enhanced ceramide synthesis and reactive oxygen species production, eventually causing cell death (38,39). In addition, the activation of peroxisome proliferator-activated receptor (PPAR) β/δ stimulates TAG accumulation in keratinocytes, which was accompanied by the stimulation of keratinocyte differentiation, improved barrier homeostatis and anti-inflammatory activity (40). However, the role of TAG accumulation remains unclear and it is not known, whether it contributes to the remaining actions of PPAR-β/δ activation (40).

We also observed that Cer level in irradiated HaCaT cells increased. It seems that NB-UVB exerts similar effect on keratinocyte lipidome as does broadband UVB, especially, with regard to Cer levels. Cer are signal transducers of a variety of cell stressors, including reactive oxygen species, cytokines, exposure to chemotherapeutic agents, irradiation or exogenous lipopolysaccharides (41). Increased Cer levels provoked cell cycle arrest and/or apoptosis in a variety of cell types (41). It was assumed that stressors can increase Cer either by accelerating sphingomyelin hydrolysis by activating a sphingomyelinase or by increased *de novo* ceramide biosynthesis via activation of either ceramide synthase or serine palmitoyltransferase (42–44). It was shown by Uchida et al. (44) and Magnoni et al. (45) that UV irradiation enhanced *de novo* ceramide synthesis in cultured keratinocytes by activating ceramide synthase.

Interestingly, we found that the content of some PC- and PE-ethers (1-alkyl,2-acylglycerophosphocholines and 1-alkyl,2-acylglycerophosphoethanolamines) also increased in irradiated cells. Although their role in irradiation response remains unclear, it is likely that was also associated with on-going apoptosis, as they changed similarly to Cer. Their highest level was achieved 12-h postirradiation and later dropped down to the basal level. It was previously reported that synthetic ether phospholipids (e.g. 1-O-octadecyl-2-O-methyl-*rac*-glycero-3-phosphocholine) were able to induce apoptosis in a number of cells (46,47).

In contrast to Carsberg et al. (48) we did not observe that NB-UVB irradiation increased the DAG level. However, Carsberg et al. (48) used the full spectrum of UV irradiance, including both UVB and UVA. It is likely that
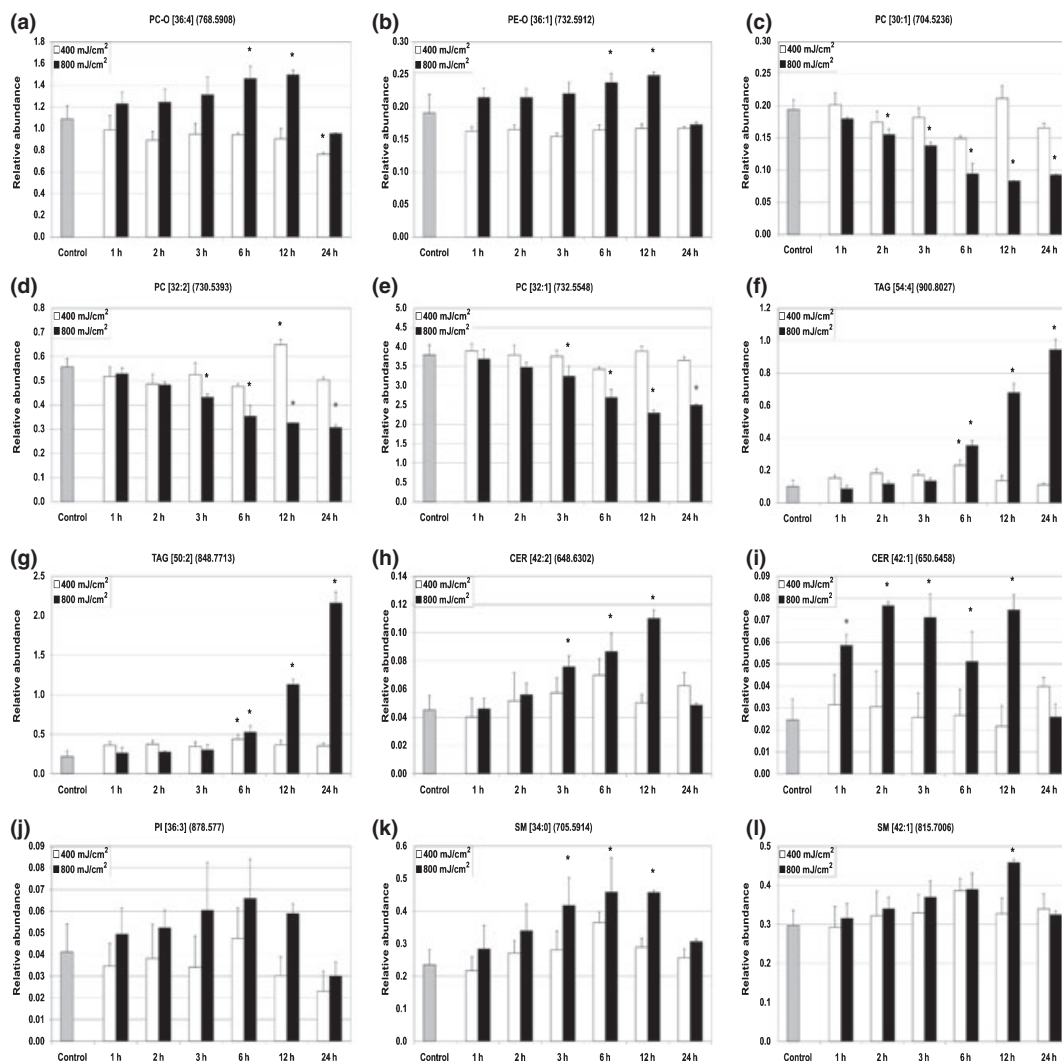
Figure 4. Comparison of selected lipid species in HaCaT cells irradiated with 400 mJ/cm² (open bars) and 800 mJ/cm² of narrow-band ultraviolet B (black bars) based on the MS/MS evaluation (*$P < 0.01$ compared with control cells): Marked increase of various PC- and PE-ethers in cells irradiated with 800 mJ/cm² (a, b) and a decrease of short chain PC-species post-NB-UVB exposure (c–e); significant raise of TAG content detected by mass spectrometry already 6-h post-NB-UVB exposure (f, g); increased abundance of Cer 42:1 and Cer 42:2 lipid species (h, i), even prior to the accumulation of TAGs.
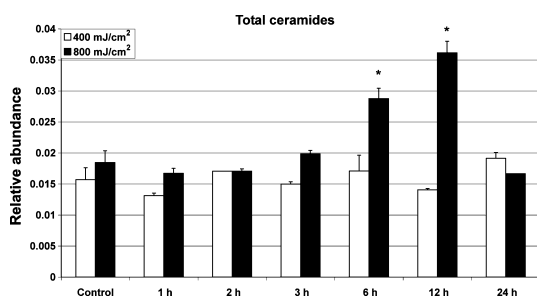
Figure 5. A total content of ceramides in irradiated cells: A maximum of ceramide levels was found at 12-h post 800 mJ/cm² NB-UVB exposure before the ceramide content again dropped to levels similar to that found in control cells (*$P < 0.05$).

increased synthesis of DAG might be related to UVA irradiation, as DAG is able to induce skin pigmentation (49), an action usually linked with UVA.

The clinical relevance of our *in vitro* experiments on immortalized cell culture still remains to be established. However, it was previously found that patients with atopic dermatitis, psoriasis or contact dermatitis have diminished skin barrier function that is related to abnormal lipid composition of stratum corneum, in which the level of Cer was decreased (50). It was also shown that topically applied emollient with Cer is effective in the treatment of atopic dermatitis (51). Hence, we speculate that NB-UVB, which is frequently used for treatment of atopic dermatitis or

psoriasis, might help to restore epidermal barrier. The healing effect could be achieved via inducing apoptosis in keratinocytes that lead to increased synthesis of Cer and TAG. This positive effect of UV irradiation has been already observed by Wefers et al. (52). Although the increase of Cer content upon single NB-UVB irradiation was observed for a short period of time, it seems that repetitive therapy with NB-UVB, as it is usually applied, may lead to durable increase of Cer and TAG levels in epidermis.

Hence, we concluded that NB-UVB at reasonable irradiation doses results in major changes in the keratinocyte lipidome, which correspond to the progressive apoptosis. However, the amount of storage lipids (TAG) and signalling lipids (Cer) alters, membrane lipidome stays intact, as evidenced by unperturbed levels of major glycerophospholipids and cholesterol.

Acknowledgements

References

1 Bissett D L, Hannon D P, Orr T V. Wavelength dependence of histological, physical, and visible changes in chronically UV-irradiated hairless mouse skin. Photochem Photobiol 1989: **50**: 763–769.
2 Van Weelden H, Young E, van der Leun J C. Therapy of psoriasis: comparison of photochemotherapy and several variants of phototherapy. Br J Dermatol 1980: **103**: 1–9.
3 Parrish J A, Jaenicke K F. Action spectrum for phototherapy of psoriasis. J Invest Dermatol 1981: **76**: 359–362.
4 Bandow G D, Koo J Y M. Narrow-band ultraviolet B radiation: a review of the current literature. Int J Dermatol 2004: **43**: 555–561.
5 Kunisada M, Kumimoto H, Ishizaki K, Sakumi K, Nakabeppu Y, Nishigori C. Narrow-band UVB induces more carcinogenic skin tumors than broad-band UVB through the formation of cyclobutane pyrimidine dimer. J Invest Dermatol 2007: **127**: 2865–2871.
6 Hearn R M, Kerr A C, Rahim K F, Ferguson J, Dawe R S. Incidence of skin cancers in 3867 patients treated with narrow-band ultraviolet B phototherapy. Br J Dermatol 2008: **159**: 931–935.
7 Macve J C, Norval M. The effects of UV waveband and cis-urocanic acid on tumour outgrowth in mice. Photochem Photobiol Sci 2002: **1**: 1006–1011.
8 Yule S, Dawe R S, Cameron H, Ferguson J, Ibbotson S H. Does narrow-band ultraviolet B phototherapy work in atopic dermatitis through a local or a systemic effect? Photodermatol Photoimmunol Photomed 2005: **21**: 333–335.
9 Ozawa M, Ferenczi K, Kikuchi T et al. 312-nanometer ultraviolet B light (narrow-band UVB) induces apoptosis of T cells within psoriatic lesions. J Exp Med 1999: **189**: 711–718.
10 Piskin G, Sylva-Steenland R M R, Bos J D, Teunissen M B M. T cells in psoriatic lesional skin that survive conventional therapy with NB-UVB radiation display reduced IFN-γ expression. Arch Dermatol Res 2004: **295**: 509–516.
11 Sigmundsdottir H, Johnston A, Gudjonsson J E, Valdimarsson H. Narrowband-UVB irradiation decreases the production of pro-inflammatory cytokines by stimulated T cells. Arch Dermatol Res 2005: **297**: 39–42.
12 Lehmann B, Knuschke P, Meurer M. UVB-induced conversion of 7-dehydrocholesterol to 1α,25-dihydroxyvitamin D₃ (calcitriol) in the human keratinocyte line HaCaT. Photochem Photobiol 2000: **72**: 803–809.
13 Lehmann B. Role of the vitamin D3 pathway in healthy and diseased skin – facts, contradictions and hypotheses. Exp Dermatol 2009: **18**: 97–108.
14 Reich A, Lehmann B, Meurer M, Muller D J. Structural alterations provoked by narrow band ultraviolet B in immortalized keratinocytes: assessment by atomic force microscopy. Exp Dermatol 2007: **16**: 1007–1015.
15 Reich A, Meurer M, Viehweg A, Muller D J. Narrow-band UVB induced externalization of selected nuclear antigens in keratinocytes: implications for lupus erythematosus pathogenesis. Photochem Photobiol 2009: **85**: 1–7.
16 Gloor M, Scherotzke A. Age dependence of ultraviolet light-induced erythema following narrow-band UVB exposure. Photodermatol Photoimmunol Photomed 2002: **18**: 121–126.
17 Aufiero B M, Talwar H, Young C et al. Narrow-band UVB induces apoptosis in human keratinocytes. J Photochem Photobiol B 2006: **82**: 132–139.
18 Punnonen K, Puntala A, Jansen C T, Ahotupa M. UVB irradiation induces lipid peroxidation and reduces antioxidant enzyme activities in human keratinocytes in vitro. Acta Derm Venereol 1991: **71**: 239–242.
19 Punnonen K, Puustinen T, Jansen C T. Ultraviolet B irradiation induces changes in the distribution and release of arachidonic acid, dihomo-gamma-linolenic acid, and eicosapentaenoic acid in human keratinocytes in culture. J Invest Dermatol 1987: **88**: 611–614.
20 Punnonen K, Yuspa S H. Ultraviolet light irradiation increases cellular diacylglycerol and induces translocation of diacylglycerol kinase in murine keratinocytes. J Invest Dermatol 1992: **99**: 221–226.
21 Magnoni C, Euclidi E, Benassi L et al. Ultraviolet B radiation induces activation of neutral and acidic sphingomyelinases and ceramide generation in cultured normal human keratinocytes. Toxicol In Vitro 2002: **16**: 349–355.
22 Boukamp P, Petrussevska R T, Breitcreutz D, Hornung J, Marham A, Fusenig N E. Normal keratinization in a spontaneously immortalized aneuploid human keratinocytes cell line. J Cell Biol 1988: **106**: 761–771.
23 Bligh E G, Dyer W J. A rapid method for total lipid extraction and purification. Can J Biochem Physiol 1959: **37**: 911–917.
24 Schürer N, Köhne A, Schliep V, Barlag K, Goerz G. Lipid composition and synthesis of HaCaT cells, an immortalized human keratinocyte line, in comparison with normal human adult keratinocytes. Exp Dermatol 1993: **2**: 179–185.
25 Dasgupta S, Hogan E L. Chromatographic resolution and quantitative assay of CNS tissue sphingoids and sphingolipids. J Lipid Res 2001: **42**: 301–308.
26 Kuerschner L, Ejsing C S, Ekroos K, Shevchenko A, Anderson K I, Thiele C. Polyene-lipids: a new tool to image lipids. Nat Methods 2005: **2**: 39–45.
27 Schwudke D, Liebisch G, Herzog R, Schmitz G, Shevchenko A. Shotgun lipidomics by tandem mass spectrometry under data-dependent acquisition control. Methods Enzymol 2007: **433**: 175–191.
28 Schwudke D, Hannich J T, Surendranath V et al. Top-down lipidomic screens by multivariate analysis of high-resolution survey mass spectra. Anal Chem 2007: **79**: 4083–4093.
29 Bonzón-Kulichenko E, Schwudke D, Gallardo N et al. Central leptin regulates total ceramide content and sterol regulatory element binding protein-1C proteolytic maturation in rat white adipose tissue. Endocrinology 2009: **150**: 169–178.
30 Finstad H S, Dyrendal H, Myhrstad M C, Heimli H, Drevon C A. Uptake and activation of eicosapentaenoic acid are related to accumulation of triacylglycerol in Ramos cells dying from apoptosis. J Lipid Res 2000: **41**: 554–563.
31 Al-Saffar N M, Titley J C, Robertson D et al. Apoptosis is associated with triacylglycerol accumulation in Jurkat T-cells. Br J Cancer 2002: **86**: 963–970.
32 Listenberger L L, Han X, Lewis S E et al. Triglyceride accumulation protects against fatty acid-induced lipotoxicity. Proc Natl Acad Sci USA 2003: **100**: 3077–3082.
33 Martins de Lima T, Cury-Boaventura M F, Giannocco G, Nunes M T, Curi R. Comparative toxicity of fatty acids on a macrophage cell line (J774). Clin Sci (Lond) 2006: **111**: 307–317.
34 Cnop M, Hannaert J C, Hoorens A, Eizirik D L, Pipeleers D G. Inverse relationship between cytotoxicity of free fatty acids in pancreatic islet cells and cellular triglyceride accumulation. Diabetes 2001: **50**: 1771–1777.
35 Healy D A, Watson R W, Newsholem P. Polyunsaturated and monounsaturated fatty acids increase neutral lipid accumulation, caspase activation and apoptosis in a neutrophil-like, differentiated HL-60 cell line. Clin Sci 2003: **104**: 171–179.
36 Williams S N O, Anthony M L, Brindle K M. Induction of apoptosis in two mammalian cell lines results in increased levels of fructose-1,6-bisphosphate and CDP-choline as determined by 31P MRS. Magn Reson Med 1998: **40**: 411–420.
37 Anthony M L, Zhao M, Brindle K M. Inhibition of phosphatidylcholine biosynthesis following induction of apoptosis in HL-60 cells. J Biol Chem 1999: **274**: 19686–19692.
38 Iturralde M, Gamen S, Pardo J et al. Saturated free fatty acid release and intracellular ceramide generation during apoptosis induction are closely related processes. Biochim Biophys Acta 2003: **1634**: 40–51.
39 Aronis A, Madar Z, Tirosh O. Mechanism of underlying oxidative stress-mediated lipotoxicity: exposure of J744.2 macrophages to triacylglycerols facilitates mitochondrial reactive oxygen species production and cellular necrosis. Free Radical Biol Med 2005: **38**: 1221–1230.
40 Schmuth M, Haqq C M, Cairns W J et al. Peroxisome proliferator-activated receptor (PPAR)-beta∕delta stimulates differentiation and lipid accumulation in keratinocytes. J Invest Dermatol 2004: **122**: 971–983.
41 Mathias S, Pena L A, Kolesnick R N. Signal transduction of stress via ceramide. Biochem J 1998: **335**: 465–480.
42 Pena L A, Fuks Z, Kolesnick R. Stress-induced apoptosis and the sphingomyelin pathway. Biochem Pharmacol 1997: **53**: 615–621.
43 Perry D K, Carton J, Shah A K, Meredith F, Uhlinger D J, Hannun Y A. Serine palmitoyltrasferase regultes de novo ceramide generation during etoposide-induced apoptosis. J Biol Chem 2000: **275**: 9078–9084.
44 Uchida Y, Di Nardo A, Collins V, Elias P M, Holleran W M. De novo ceramide synthesis participates in the ultraviolet B irradiation-induced apoptosis in undifferentiated cultured human keratinocytes. J Invest Dermatol 2003: **120**: 662–669.

45 Magnoni C, Euclidi E, Benassi L et al. Ultraviolet B radiation induces activation of neutral and acidic sphingomyelinases and ceramide generation in cultured normal human keratinocytes. Toxicol in Vitro 2002: **16**: 349–355.

46 Verdonck LF, van Heugten HG. Ether lipids are effective cytotoxic drugs against multidrug-resistant acute leukemia cells and can act by the induction of apoptosis. Leuk Res 1997: **21**: 37–43.

47 Cabaner C, Gajate C, Macho A, Muñoz E, Modolell M, Mollinedo F. Induction of apoptosis in human mitogen-activated peripheral blood T-lymphocytes by the ether phospholipid ET-18-OCH3: involvement of the Fas receptor/ligand system. Br J Pharmacol 1999: **127**: 813–825.

48 Carsberg CJ, Ohanian J, Friedmann PS. Ultraviolet radiation stimulates a biphasic pattern of 1,2-diacylglycerol formation in cultured human melanocytes and keratinocytes by activation of phospholipases C and D. Biochem J 1995: **305**: 471–477.

49 Gordon PR, Gilchrest BA. Human melanogenesis is stimulated by diacylglycerol. J Invest Dermatol 1989: **93**: 700–702.

50 Choi MJ, Maibach HI. Role of ceramides in barrier function of healthy and diseased skin. Am J Clin Dermatol 2005: **6**: 215–223.

51 Chamlin SL, Kao J, Frieden IJ et al. Ceramide-dominant barrier repair lipids alleviate childhood atopic dermatitis: changes in barrier function provide a sensitive indicator of disease activity. J Am Acad Dermatol 2002: **47**: 198–208.

52 Wefers H, Melnik BC, Flür M, Bluhm C, Lehmann P, Plewig G. Influence of UV irradiation on the composition of human stratum corneum lipids. J Invest Dermatol 1991: **96**: 959–962.

Supporting information

Additional Supporting Information may be found in the online version of this article:

Figure S1. Lipid composition of HaCaT cells after irradiation with 400 mJ/cm^2 of NB-UVB as demonstrated by thin layer chromatography (TLC) after running two-thirds of the separation distance in chloroform/ethanol/water/triethylamine (35:40:9:35), and subsequently separated in *n*-hexane/ethylacetate (5:1) (left: original TLC plate scan, right: graphic representations of selected samples as indicate on the TLC plate): No significant changes in major lipid classes were found by TLC in keratinocytes irradiated with 400 mJ/cm^2 of NB-UVB. (Card, cardiolipin; Cer, ceramides; ChE, cholesterol esters; Chol, cholesterol; DAG, diacylglycerols; FFA, free fatty acids; Glc-Cer, glucosyl ceramides; PA, phosphatidic acid; PC, phosphatidylcholine; PE, phosphatidylethanolamine; PI, phosphatidylinositol; PS, phosphatidylserine; SM, sphingomyelin; TAG, triacylglycerols).

Table S1. (a) Major lipid classes in HaCaT cell line before and after narrow-band UVB irradiation with 400 mJ/cm^2 based on assessment of thin layer chromatography: no significant differences (*P*-values according to analysis of variance and *post hoc* analysis with Tukey honest significance test; Card, cardiolipin; Cer, ceramides; ChE, cholesterol esters; Chol, cholesterol; DAG, diacylglycerols; FFA, free fatty acids; Glc-Cer, glucosyl ceramides; PA, phosphatic acid; PC, phosphatidylcholine; PE, phosphatidylethanolamine; PI, phosphatidylinositol; PS, phosphatidylserine; SM, sphingomyelin; TAG, triacylglycerols). (b) Major lipid classes in HaCaT cell line before and after narrow-band UVB irradiation with 800 mJ/cm^2 based on assessment of thin layer chromatography: *significant difference between total TAG content 24-h postirradiation compared to the rest of measurements of TAG level, **significant difference of total PI content between baseline value and 24-h postirradiation, ***significant difference between total SM content 24-h postirradiation compared to values marked in bold (*P*-values according to analysis of variance and *post hoc* analysis with Tukey's honest significance test; Card, cardiolipin; Cer, ceramides; ChE, cholesterol esters; Chol, cholesterol; DAG, diacylglycerols; FFA, free fatty acids; Glc-Cer, glucosyl ceramides; PA, phosphatic acid; PC, phosphatidylcholine; PE, phosphatidylethanolamine; PI, phosphatidylinositol; PS, phosphatidylserine; SM, sphingomyelin; TAG, triacylglycerols).

Table S2. Relative abundance of lipids identified by Lipidomics Screen (results demonstrated as means ± standard deviations, sorting according to *P*-values based on analysis of variance; rows marked in bold demonstrated on Fig. 4).

Please note: Wiley-Blackwell are not responsible for the content or functionality of any supporting materials supplied by the authors. Any queries (other than missing material) should be directed to the corresponding author for the article.